

CROSS-POINTS IN DOMAIN DECOMPOSITION METHODS WITH A FINITE ELEMENT DISCRETIZATION*

MARTIN J. GANDER[†] AND KÉVIN SANTUGINI[‡]

Abstract. Non-overlapping domain decomposition methods necessarily have to exchange Dirichlet and Neumann traces at interfaces in order to allow for convergence to the underlying mono-domain solution. Well-known such non-overlapping methods are the Dirichlet-Neumann method, the FETI and Neumann-Neumann methods, and optimized Schwarz methods. For all these methods, cross-points in the domain decomposition configuration where more than two subdomains meet do not pose any problem at the continuous level, but care must be taken when the methods are discretized. We show in this paper two possible approaches for the consistent discretization of Neumann conditions at cross-points in a finite element setting: the *auxiliary variable method* and *complete communication*.

Key words. domain decomposition, cross-points, finite element discretization, auxiliary variables, complete communication

AMS subject classifications. 65N55, 65N30, 65F10

1. Introduction. Domain decomposition methods (DDMs) are among the best parallel solvers for elliptic partial differential equations; see the books [29, 30, 32] and references therein. While classical Schwarz methods only exchange Dirichlet information from subdomain to subdomain and converge because of overlap, non-overlapping methods like Dirichlet-Neumann, FETI, Neumann-Neumann, and optimized Schwarz methods (OSMs) also exchange Neumann traces or combinations of Dirichlet and Neumann traces between subdomains. In a general decomposition of a domain $\Omega \subset \mathbb{R}^2$ into non-overlapping subdomains $(\Omega_i)_{1 \leq i \leq I}$, naturally cross-points arise. Such cross-points, where more than two subdomains meet, do not pose any problem in a continuous variational setting, but as soon as one introduces a finite-dimensional approximation, the discretization of a Neumann condition over a cross-point does not follow naturally. The earliest paper dedicated to cross-points dates, to our knowledge, back to 1986: in [8], a Dirichlet-Neumann method is presented for domain decompositions with Cartesian topology that can be colored with only two colors. Boundary points, including cross-points, are part of the Neumann subdomains, and all Neumann subdomains are coupled at cross-points while Dirichlet subdomains are fully decoupled. In [2], a Krylov-accelerated DDM to compute the collocation solution of the Poisson equation in a square with Hermite finite elements is studied. There are four subdomains in a 2×2 grid configuration, thus involving a cross-point, and theoretical convergence estimates are provided. The FETI-DP algorithm [9, 25] modifies the FETI algorithm [28] at cross-points by replacing the dual variables by primal ones and thus avoiding the problem of Neumann conditions there. Similarly, strong coupling at cross-points is also proposed in [1, 3] for nodal finite elements. In [14], it was shown for OSMs in an algebraic setting that optimized Robin parameters scale differently at cross-points, namely like $O(1/h)$ in contrast to $O(1/\sqrt{h})$ at interface points which are not cross-points; see also [27] for condition number estimates in the presence of cross-points. Cross-points can also be handled in the context of mortar methods, and in very special symmetric configurations, it is actually possible for cross-points not to pose any problems; see [15]. The cross-point problem can be avoided entirely when using cell-centered finite volume discretizations because they do not contain cross-points at the

*Received April 18, 2014. Accepted March 17, 2016. Published online on June 15, 2016. Recommended by A. Klawonn.

[†]Université de Genève, Section de Mathématiques, Geneva, Switzerland (Martin.Gander@unige.ch).

[‡]Bordeaux INP, IMB, UMR 5251, F-33400, Talence, France
(Kevin.Santugini-Repiquet@bordeaux-inp.fr).

discrete level; see [4] for the convergence of the cell-centered finite volume OSM with Robin transmission conditions, see [19] for the convergence of the cell-centered finite volume OSM with Ventcell transmission conditions in the absence of cross-points and [16] for the extension of the convergence proof to symmetric positive definite transmission operators even in the presence of cross-points.

We describe in this paper in detail two approaches to exchange Neumann traces over cross-points in a finite element setting for two-dimensional problems: the *auxiliary variable method* and *complete communication*. The auxiliary variable method keeps in addition to the primal unknowns also auxiliary unknowns representing interface data in each subdomain. These auxiliary variables permit a consistent discretization of the Neumann traces at cross-points while only communicating with neighboring domains that share a boundary of non-zero one-dimensional measure. As a first main result, we show that with auxiliary variables, one can prove convergence of the discretized DDM using energy estimates, which is not possible for finite element discretizations with cross-points otherwise [15]. A disadvantage of the auxiliary variables is that they are not necessarily converging to a limit, but this does not affect the convergence of the primal unknowns in the iteration; see Section 3.2. Complete communication needs to exchange information with all subdomains touching at cross-points, also those which touch only at a point, in order to have a consistent discretization of Neumann conditions. Our second main result answers the question of how to determine for complete communication a splitting of Neumann traces that minimizes oscillation among the many possible ones.

Our paper is organized as follows: in Section 2, we describe for the concrete example of an OSM why the discretization of the Neumann part of the transmission condition is ambiguous at cross-points. In Section 3, we present the first approach to how to transmit Neumann information near cross-points using auxiliary variables and give a general convergence proof for a non-overlapping OSM discretized by finite elements with cross-points. In Section 4, we describe how Neumann information can be transmitted near cross-points by complete communication among all subdomains sharing the cross-point, and we propose a specific method minimizing oscillation. After our conclusions in Section 5, we show in Appendix A that instead of using higher-order, so-called Ventcell transmission conditions (see for example [5, 10, 12, 21, 22, 23, 24]), one can obtain algebraically naturally such conditions from Robin conditions using mass lumping techniques in a finite element setting. This avoids the need for discretizing higher-order differential operators in the tangential direction and even works at cross-points, which is our third important result.

2. The discrete optimized Schwarz method. For the elliptic problem $\mathcal{L}u = f$ in Ω and a non-overlapping decomposition $(\Omega_i)_{1 \leq i \leq I}$, the OSM with Robin transmission conditions at the continuous level is (see for example [10]):

ALGORITHM 2.1 (OSM).

1. Set $p > 0$.
2. Start with an initial guess u_i^0 in each subdomain Ω_i .
3. Until convergence, compute for $n = 0, 1, \dots$, in parallel the unique solution u_i^{n+1} to

$$(2.1) \quad \begin{aligned} \mathcal{L}u_i^{n+1} &= f && \text{in } \Omega_i, \\ \frac{\partial u_i^{n+1}}{\partial \mathbf{n}_{ii'}} + pu_i^{n+1} &= \frac{\partial u_{i'}^n}{\partial \mathbf{n}_{ii'}} + pu_{i'}^n && \text{on } \partial\Omega_i \cap \partial\Omega_{i'}, \end{aligned}$$

where $\mathbf{n}_{i,i'}$ is the normal to $\partial\Omega_i \cap \partial\Omega_{i'}$ pointing from Ω_i to $\Omega_{i'}$.

In a variational formulation of Algorithm 2.1, cross-points do not pose any problem since they have zero measure. In a finite-dimensional approximation however, using for example

finite elements, the Neumann part of the Robin transmission conditions is only known as a variational quantity, i.e., as an integral over the edges connected to the cross-point. When discretizing an OSM (or any DDM), one should strive to make the DDM consistent at the discrete level:

DEFINITION 2.2 (Consistent Discrete DDM). *A discrete DDM is called consistent if*

1. *the discrete mono-domain solution is a fixed-point of the discrete DDM,*
2. *the discrete DDM has a unique fixed-point.*

We show in this section that it is not completely straightforward to design a consistent discrete iterative DDM when cross-points are present.

2.1. Geometric setting and notation. Let \mathcal{T} be a polygonal mesh of $\Omega \subset \mathbb{R}^2$. Let $(\Omega_i)_{1 \leq i \leq I}$ be a non-overlapping partition of the domain Ω . We assume that the subdomains Ω_i are polygonal and that each cell of \mathcal{T} is included in exactly one subdomain. Let \mathcal{T}_i be the restriction of the mesh \mathcal{T} to Ω_i , and denote by \mathbf{x}_j the vertices of the mesh \mathcal{T} . We consider a finite element space $\mathcal{P}(\mathcal{T})$ being a subset of $H_0^1(\Omega)$ with the following properties:

1. There is exactly one degree of freedom at each vertex of \mathcal{T} for $\mathcal{P}(\mathcal{T})$.
2. For any edge $[\mathbf{x}_j \mathbf{x}_{j'}]$ of $\mathcal{P}(\mathcal{T})$ and for any u in $\mathcal{P}(\mathcal{T})$, $u(\mathbf{x}_j) = 0$ and $u(\mathbf{x}_{j'}) = 0$ imply that u vanishes on the entire edge $[\mathbf{x}_j \mathbf{x}_{j'}]$.

Both of these conditions are satisfied for P_1 -elements on triangular meshes and Q_1 -elements on Cartesian ones. We define $\mathcal{P}(\mathcal{T}_i) := \{u|_{\Omega_i} | u \in \mathcal{P}(\mathcal{T})\}$. We denote the hat-functions by ϕ_j , i.e., the unique function in $\mathcal{P}(\mathcal{T})$ such that

$$\phi_j(\mathbf{x}_{j'}) = \begin{cases} 1 & \text{if } j = j', \\ 0 & \text{if } j \neq j', \end{cases}$$

and by $\phi_{i;j}$ we denote $(\phi_j)|_{\Omega_i}$. We will systematically use the letter i for subdomain indices and separate it from nodal indices j using a semicolon. The discretized OSM operates then on the space

$$V := \bigotimes_{i=1}^N \mathcal{P}(\mathcal{T}_i).$$

Since a node located on a subdomain boundary may belong to more than one subdomain, we use the index i in $\mathbf{x}_{i;j}$ to distinguish degrees of freedom located at the same node but belonging to different subdomains.

2.2. Discretization of Robin transmission conditions. The discrete Neumann boundary condition must be computed variationally in an FEM setting; see for example [32, p. 3, equation (1.7)]. Near cross-points, the Neumann boundary condition is similar to an integral over both edges that are adjacent to the cross-point and belong to the boundary of the subdomain. As there is no canonical way to split that variational Neumann boundary condition, it is not clear how we should split that quantity when it comes to transmitting Neumann information between adjacent subdomains near cross-points. Any splitting should be consistent according to Definition 2.2.

To investigate this problem, it suffices to study the case of the elliptic operator $\mathcal{L} := \eta - \Delta$, $\eta > 0$, in Algorithm 2.1 with homogenous Dirichlet boundary conditions on $\partial\Omega$. Since we want to study the consistency of an iterative discrete DDM according to Definition 2.2, we first need to specify the mono-domain solution. Following finite element principles, we need to solve

$$\eta \int_{\Omega} u \phi_j + \int_{\Omega} \nabla u \cdot \nabla \phi_j = \int_{\Omega_i} f \phi_j,$$

where $u = \sum_j u_j^{n+1} \phi_j$. If we define the matrix \mathbf{A} by

$$A_{j,j'} := \eta \int_{\Omega} \phi_j(\mathbf{x}) \phi_{j'}(\mathbf{x}) d\mathbf{x} + \int_{\Omega} \nabla \phi_j(\mathbf{x}) \nabla \phi_{j'}(\mathbf{x}) d\mathbf{x},$$

then the discrete mono-domain equation is

$$(2.2) \quad \mathbf{A} \mathbf{u} = \mathbf{f},$$

where the components of \mathbf{f} satisfy $f_j = \int_{\Omega_i} f \phi_j$ for every nodal index j .

In the discrete OSM, at every new iteration $n + 1$, following finite element principles, we solve for every subdomain Ω_i the equation

$$(2.3) \quad \eta \int_{\Omega_i} u_i^{n+1} \phi_{i;j} + \int_{\Omega_i} \nabla u_i^{n+1} \cdot \nabla \phi_{i;j} + p \int_{\partial\Omega_i} u_i^{n+1} \phi_{i;j} d\sigma(\mathbf{x}) = f_{i;j} + g_{i;j}^{n+1}$$

for all j such that $\mathbf{x}_{i;j}$ is a node of mesh \mathcal{T} located in $\bar{\Omega}_i$, in order to find the new finite element subdomain solution approximation by $u_i^{n+1} = \sum_j u_{i;j}^{n+1} \phi_{i;j}$. The data $g_{i;j}^{n+1}$ needs to be gathered from neighboring subdomains satisfying (2.1) in a discrete sense which makes the discrete OSM consistent according to Definition 2.2. We will see that this means computing the Neumann contribution to $g_{i;j}^{n+1}$ variationally, i.e., using (2.8) and (2.9). We denote by the matrix \mathbf{A}_i the sum of the mass and stiffness contributions corresponding to the interior equation $\eta - \Delta$ in each subdomain Ω_i ,

$$(2.4) \quad A_{i;j,j'} := \eta \int_{\Omega_i} \phi_{i;j}(\mathbf{x}) \phi_{i;j'}(\mathbf{x}) d\mathbf{x} + \int_{\Omega_i} \nabla \phi_{i;j}(\mathbf{x}) \nabla \phi_{i;j'}(\mathbf{x}) d\mathbf{x}.$$

The matrix $\mathbf{B}_i^{\text{cons}}$ contains the boundary contribution $p \int_{\partial\Omega_i} u_i^{n+1} \phi_{i;j} d\sigma(\mathbf{x})$ including the Robin parameter p : if the finite elements are linear on each edge, which holds for Q_1 - and P_1 -elements, we have the consistent interface mass matrix

$$(2.5) \quad B_{i;j,j'}^{\text{cons}} := \begin{cases} \frac{p}{3} \sum_{j''} |\mathbf{x}_{i;j} - \mathbf{x}_{i;j''}| & \text{if } j' = j \text{ and } \mathbf{x}_{i;j} \text{ lies on } \partial\Omega_i, \\ \frac{p}{6} |\mathbf{x}_{i;j} - \mathbf{x}_{i;j'}| & \text{if } [\mathbf{x}_{i;j} \mathbf{x}_{i;j'}] \text{ is an edge of } \partial\Omega_i, \\ 0 & \text{otherwise,} \end{cases}$$

where the sum is taken over all $j'' \neq j$ such that $[\mathbf{x}_j \mathbf{x}_{j''}]$ is a boundary edge of \mathcal{T}_i . A lumped version of the interface mass matrix $\mathbf{B}_i^{\text{cons}}$ is

$$(2.6) \quad B_{i;j,j'}^{\text{lump}} := \begin{cases} \frac{p}{2} \sum_{j''} |\mathbf{x}_{i;j} - \mathbf{x}_{i;j''}| & \text{if } j = j' \text{ and } \mathbf{x}_{i;j} \text{ lies on } \partial\Omega_i, \\ 0 & \text{otherwise,} \end{cases}$$

where again the sum is taken over all $j'' \neq j$ such that $[\mathbf{x}_j \mathbf{x}_{j''}]$ is a boundary edge of \mathcal{T}_i . We explain in Appendix A why using a lumped interface mass matrix $\mathbf{B}_i^{\text{lump}}$ leads to faster convergence than using a consistent mass matrix $\mathbf{B}_i^{\text{cons}}$ by interpreting the lumping process at the continuous level as introducing a higher-order term in the transmission condition; see also [7]. This higher-order term can even be optimized using a new concept of overlumping which we introduce in this paper in Appendix A. Note that in the context of discrete duality finite volume methods, it was shown in [13] that the consistent mass matrix can even completely destroy the asymptotic performance of the OSM even without cross-points. This is however not the case for the finite element discretizations we consider here. To simplify notations and shorten formulas, we only consider the lumped Robin boundary conditions throughout the rest

of this paper except in Appendix A, where we also consider consistent and overlumped Robin boundary conditions.

Using the matrix notation that we introduced, we have to solve at each Schwarz iteration a matrix problem equivalent to (2.3), namely

$$(2.7) \quad (\mathbf{A}_i + \mathbf{B}_i^{\text{lump}}) \mathbf{u}_i^{n+1} = \mathbf{f}_i + \mathbf{g}_i^{n+1},$$

where the vector \mathbf{g}_i^{n+1} is zero at interior nodes of Ω_i and contains the values $g_{i,i'}^n$ transmitted from the neighboring subdomains $\Omega_{i'}$ to the interface nodes of Ω_i . The computation of \mathbf{f}_i and \mathbf{g}_i^{n+1} should be done in such a way that the discrete DDM is consistent according to Definition 2.2. At the continuous level, \mathbf{f}_i would just be the restriction of f to Ω_i , and hence, if the continuous function f is known, one can set

$$f_{i;j} := \int_{\Omega_i} f(\mathbf{x}) \phi_{i;j} d\mathbf{x}.$$

In some cases, the right-hand side f is not known at the continuous level, and only the right-hand side \mathbf{f} of the discrete mono-domain equation (2.2) is given. In such cases, one has to choose a decomposition of \mathbf{f} into the right-hand sides \mathbf{f}_i of the local subdomain problems (2.7). Such a decomposition $(\mathbf{f}_i)_{1 \leq i \leq I}$ should satisfy $f_j = \sum_i f_{i;j}$ for each nodal index j , and the sum is over all indices i such that \mathbf{x}_j belongs to $\bar{\Omega}_i$. For the transmitted values $g_{i,i'}^n$ with a finite element discretization, the Neumann contribution must be defined by a variational problem for the discrete mono-domain solution to be a fixed-point of the discrete OSM iteration. At the continuous level, if $(\eta - \Delta)u_i = f$ inside Ω_i , we have by Green's formula

$$\int_{\partial\Omega_i} \frac{\partial u_i}{\partial \mathbf{n}_i} v = \eta \int_{\Omega_i} uv + \int_{\Omega_i} \nabla u \nabla v - \int_{\Omega_i} f v.$$

This formula must be used to define discrete Neumann boundary conditions: for $\mathbf{x}_{i;j}$ a vertex of the fine mesh located on $\partial\Omega_i$, we define, for every w_i in $\mathcal{P}(\mathcal{T}_i)$ that satisfies $(\mathbf{A}_i \mathbf{w}_i)_{i;j} = f_{i;j}$ at every interior node \mathbf{x}_j of \mathcal{T}_i , the Neumann quantity

$$(2.8) \quad \mathcal{N}_{i;j}(w_i) := \eta \int_{\Omega_i} w_i \phi_{i;j} + \int_{\Omega_i} \nabla w_i \nabla \phi_{i;j} - f_{i;j}$$

for every boundary node \mathbf{x}_j of \mathcal{T}_i . The discrete mono-domain solution satisfies the identity $\sum_i \mathcal{N}_{i;j}(u_i) = 0$, where the sum is over all i such that \mathbf{x}_j is a boundary vertex of \mathcal{T}_i . This is the discrete equivalent of the condition that the continuous solution does not have jumps in the Neumann traces. For interface points \mathbf{x}_j that belong to exactly two subdomains $\bar{\Omega}_i$ and $\bar{\Omega}_{i'}$, the Robin update is not ambiguous, and we set

$$(2.9) \quad g_{i,i';j}^n := -\mathcal{N}_{i';j}(u_{i'}^n) + \frac{p}{2} u_{i';j}^n \sum_{j'} |\mathbf{x}_{i;j} - \mathbf{x}_{i';j'}|,$$

where the sum is over all j' such that $[\mathbf{x}_j \mathbf{x}_{j'}]$ is a boundary edge of both \mathcal{T}_i and $\mathcal{T}_{i'}$. The subdomain $\Omega_{i'}$ must then send $g_{i,i';j}^n$ to the subdomain Ω_i , which uses it for its transmission condition $g_{i,i';j}^{n+1} = g_{i,i';j}^n$ since there is only one contribution from the unique neighbor $\Omega_{i'}$.

2.3. Ambiguity of the Robin update at cross-points. To see why the Robin update (2.9) cannot be used at cross-points, consider as an example the cross-point \mathbf{x}_1 belonging to the subdomain Ω_1 shown in Figure 2.1. Following (2.9), to compute g_1^{n+1} at cross-point \mathbf{x}_1 , one would intuitively set

$$g_{1;1}^{n+1} = -\mathcal{N}_{2;13}(u_2^n) + \frac{p}{2} |\mathbf{x}_1 - \mathbf{x}_3| u_{2;1}^n - \mathcal{N}_{5;12}(u_5^n) + \frac{p}{2} |\mathbf{x}_1 - \mathbf{x}_2| u_{5;1}^n,$$

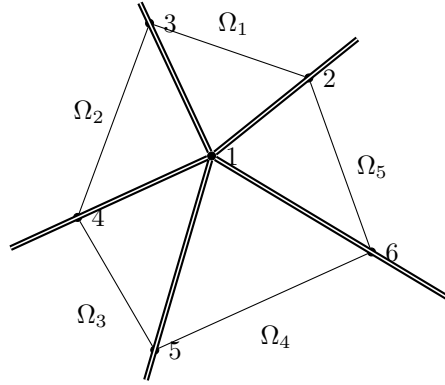


FIG. 2.1. Example of a cross-point in the decomposition.

where $\mathcal{N}_{2;13}$ is the part of $\mathcal{N}_{2;1}$ located on the edge $[\mathbf{x}_1 \mathbf{x}_3]$ and likewise for $\mathcal{N}_{5;12}$. Unfortunately, at the discrete level, the Neumann contributions of u_2^n and u_5^n at \mathbf{x}_1 are only known as an integral over the edges coming from \mathbf{x}_1 . We cannot distinguish the contribution of each edge to the Neumann conditions $\mathcal{N}_{2;1}(u_2^n)$ and $\mathcal{N}_{5;1}(u_5^n)$. We only know that

$$\mathcal{N}_{2;1}(u_2^n) = \mathcal{N}_{2;13}(u_2^n) + \mathcal{N}_{2;14}(u_2^n), \quad \mathcal{N}_{5;1}(u_5^n) = \mathcal{N}_{5;12}(u_5^n) + \mathcal{N}_{5;16}(u_5^n).$$

When transmitting the Robin condition at a cross-point, the Neumann contribution must be split across each edge in such a way that the discrete mono-domain solution remains a fixed-point of the OSM; see item 1 in Definition 2.2. The discrete mono-domain solution satisfies

$$(2.10) \quad u_{i;j} = u_{i';j} \quad \text{for all } i' \text{ with } \mathbf{x}_j \text{ in } \Omega_{i'}, \text{ and} \quad \sum_{i, \mathbf{x}_j \in \partial\Omega_i} \mathcal{N}_{i;j}(u_i) = 0.$$

The discrete algorithm should therefore split the Neumann contributions at cross-points in such a way that whenever (2.10) holds, we have reached a fixed-point of the discrete algorithm. We show in the next two sections that such a splitting can either be obtained using auxiliary variables and communicating only with neighbors or by communicating with all subdomains that share the cross-point.

3. Auxiliary variable method. We now show how to introduce auxiliary variables near the cross-points to resolve the ambiguity. At the continuous level, we have on the interface between the subdomain Ω_i and $\Omega_{i'}$ from (2.1) the identity

$$g_i^{n+1} = \frac{\partial u_i^{n+1}}{\partial \mathbf{n}_{ii'}} + pu_i^{n+1} = \frac{\partial u_{i'}^n}{\partial \mathbf{n}_{ii'}} + pu_{i'}^n = -\frac{\partial u_{i'}^n}{\partial \mathbf{n}_{i'i}} + pu_{i'}^n = -g_{i'}^n + 2pu_{i'}^n,$$

since by definition $g_{i'}^n = \frac{\partial u_{i'}^n}{\partial \mathbf{n}_{i'i}} + pu_{i'}^n$ and the normals are in opposite directions. At the discrete level, as long as we are away from cross-points, the same equality can be used to update the Robin transmission conditions,

$$(3.1) \quad g_{i;j}^{n+1} = -g_{i';j}^n + pu_{i';j}^n \sum_{j'} |\mathbf{x}_{i;j} - \mathbf{x}_{i';j'}|,$$

where the sum¹ is over all j' such that $[\mathbf{x}_j \mathbf{x}_{j'}]$ is a boundary edge of \mathcal{T}_i and the factor 2 is cancelled with the factor 1/2 in formula (2.9). This is very useful in practice because one then

¹For two-dimensional edges, there are only two terms in the sum.

does not even need to implement a normal derivative evaluation [17]. At interface points which are not cross-points, this update will give the same update as applying formula (2.9) using the definition of the discrete Neumann condition (2.8). Inspired by the update formula (3.1), we introduce the following update of the discrete Robin transmission conditions at cross-points:

ALGORITHM 3.1 (Discrete OSM with auxiliary variables).

1. Initialize $g_{i,i';j}^0$ for all nodes \mathbf{x}_j that are boundary nodes of both \mathcal{T}_i and $\mathcal{T}_{i'}$.
2. For $n = 0, 1, 2, \dots$, until convergence do
 - (a) Compute

$$(3.2) \quad g_{i;j}^{n+1} = \sum_{i'} g_{i,i';j}^n$$

where the sum is over all subdomains $\Omega_{i'}$ such that there exists an edge originating from the vertex \mathbf{x}_j that belongs to both \mathcal{T}_i and $\mathcal{T}_{i'}$.

- (b) Solve² for each subdomain Ω_i

$$(\mathbf{A}_i + \mathbf{B}_i^{lump})\mathbf{u}_i^{n+1} = \mathbf{f}_i + \mathbf{g}_i^{n+1},$$

where \mathbf{A}_i and \mathbf{B}_i^{lump} are defined in (2.6) and (2.4).

- (c) Set

$$(3.3) \quad g_{i',i;j}^{n+1} := -g_{i,i';j}^n + pu_{i;j}^{n+1} \sum_{j'} |\mathbf{x}_{i;j} - \mathbf{x}_{i';j'}|,$$

where the sum is over all j' such that $[\mathbf{x}_j \mathbf{x}_{j'}]$ is a boundary edge of both \mathcal{T}_i and $\mathcal{T}_{i'}$.

Algorithm 3.1 requires storing the auxiliary variables $g_{i',i;j}^n$ because it is not possible to recover $g_{i',i;j}^n$ from u_i^n when \mathbf{x}_j is a cross-point. Only the sum over i' of $g_{i',i;j}^n$ can be recovered from u_i^n .

3.1. Convergence of the auxiliary variable method. At the continuous level, one can prove convergence of the OSM using energy estimates; see for example [6, 26]. At the discrete level, this technique fails in general [15] precisely because of the cross-points. In this section, we prove convergence of the discrete OSM in the presence of cross-points when auxiliary variables are used, i.e., convergence of Algorithm 3.1.

To do so, we first need to prove that the discrete mono-domain solution is a fixed-point of Algorithm 3.1. We thus need to introduce the splitting of the discrete Neumann conditions at the cross-points induced by the splitting of the Robin interface conditions at cross-points: we set

$$(3.4) \quad \mathcal{N}_{i,i';j}^{n+1} := g_{i,i';j}^n - \frac{p}{2} \left(\sum_{j'} |\mathbf{x}_j - \mathbf{x}_{j'}| \right) u_{i;j}^{n+1},$$

where the sum is over all j' such that $[\mathbf{x}_j \mathbf{x}_{j'}]$ is a boundary edge of both \mathcal{T}_i and $\mathcal{T}_{i'}$. By (2.6), (2.8), and (2.7), we obtain

$$(3.5) \quad \mathcal{N}_{i;j}(u_i^{n+1}) = \sum_{i'} \mathcal{N}_{i,i';j}^{n+1},$$

²For the sake of simplicity, we only write the algorithm for lumped boundary conditions.

where the sum is over all i' such that there exists an edge originating from \mathbf{x}_j that is a boundary edge of both \mathcal{T}_i and $\mathcal{T}_{i'}$.

LEMMA 3.2. *Let $\mathbf{f} = (f_j)$ be a right-hand side of the discretized operator $\eta - \Delta$ with $f_{i;j}$ such that $\sum_i f_{i;j} = f_j$. Then there exist values $g_{i,i';j}$ which are a fixed-point of the discrete OSM with auxiliary variables near cross-points.*

Proof. Let \mathbf{u} be the discrete mono-domain solution. Let \mathbf{u}_i be the restriction of \mathbf{u} to \mathcal{T}_i . We define two sets of nodes: $\mathcal{E}_{i;j}$ is the set of all nodal indices j' such that \mathbf{x}_j and $\mathbf{x}_{j'}$ are endpoints of a boundary edge of \mathcal{T}_i , and $\mathcal{E}_{i,i';j}$ is the set of all nodal indices j' such that \mathbf{x}_j and $\mathbf{x}_{j'}$ are endpoints of a boundary edge of both \mathcal{T}_i and $\mathcal{T}_{i'}$, i.e.,

$$\begin{aligned}\mathcal{E}_{i;j} &:= \{j', [\mathbf{x}_j \mathbf{x}_{j'}] \text{ boundary edge of } \mathcal{T}_i\}, \\ \mathcal{E}_{i,i';j} &:= \{j', [\mathbf{x}_j \mathbf{x}_{j'}] \text{ boundary edge of } \mathcal{T}_i \text{ and of } \mathcal{T}_{i'}\}.\end{aligned}$$

We use formula (2.8) to obtain the existence of values $g_{i;j}$ such that the solution of (2.7) is \mathbf{u}_i . For any given cross-point node \mathbf{x}_j , we have to split the variables $g_{i;j}$ into $g_{i,i';j}$ that satisfy

$$\begin{aligned}g_{i;j} &= \sum_{i' \text{ s.t. } \mathcal{E}_{i,i';j} \neq \emptyset} g_{i,i';j}, \\ g_{i',i;j} &= -g_{i,i';j} + pu_j \sum_{j' \in \mathcal{E}_{i,i';j}} |\mathbf{x}_{i,j} - \mathbf{x}_{i,j'}|.\end{aligned}$$

Subtracting the Dirichlet parts on both sides in the first equation and transferring half the Dirichlet part in the second equation from the right to the left, we get

$$\begin{aligned}g_{i;j} - \frac{p}{2}u_j \sum_{j' \in \mathcal{E}_{i;j}} |\mathbf{x}_{i,j} - \mathbf{x}_{i,j'}| &= \sum_{i' \text{ s.t. } \mathcal{E}_{i,i';j} \neq \emptyset} (g_{i,i';j} - \frac{p}{2}u_j \sum_{j' \in \mathcal{E}_{i,i';j}} |\mathbf{x}_{i,j} - \mathbf{x}_{i,j'}|), \\ g_{i',i;j} - \frac{p}{2}u_j \sum_{j' \in \mathcal{E}_{i,i';j}} |\mathbf{x}_{i,i',j} - \mathbf{x}_{i,j'}| &= -(g_{i,i';j} - \frac{p}{2}u_j \sum_{j' \in \mathcal{E}_{i,i';j}} |\mathbf{x}_{i,j} - \mathbf{x}_{i,j'}|).\end{aligned}$$

We recognize the discrete Neumann conditions; see (3.4). So the problem becomes that of the concrete splitting problem of Neumann conditions: given $\mathcal{N}_{i;j}$, find $\mathcal{N}_{i,i';j}$ such that

$$\mathcal{N}_{i;j} = \sum_{i' \text{ s.t. } \mathcal{E}_{i,i';j} \neq \emptyset} \mathcal{N}_{i,i';j}, \quad \mathcal{N}_{i,i';j} = -\mathcal{N}_{i',i;j}.$$

By (2.10), since \mathbf{u} is the discrete mono-domain solution, we have $\sum_i \mathcal{N}_{i;j} = 0$. For each cross-point \mathbf{x}_j , we define a graph G whose set of vertices $V(G)$ and set of edges $E(G)$ are defined as

$$\begin{aligned}V(G) &= \{i, \mathbf{x}_j \in \bar{\Omega}_i\}, \\ E(G) &= \{\{i, i'\} \subset V(G), \mathcal{T}_i \text{ and } \mathcal{T}_{i'} \text{ share an edge originating from } \mathbf{x}_j\}.\end{aligned}$$

We set $\phi(i) := \mathcal{N}_{i;j}$ for all i in $V(G)$ and apply Lemma B.1. Setting $\mathcal{N}_{i,i',j} = \psi(i, i')$ from Lemma B.1 for all (i, i') in $E(G)$ then concludes the proof. \square

THEOREM 3.3. *The OSM, Algorithm 2.1, discretized with finite elements (2.3) and using auxiliary variables for the transmission conditions is convergent.*

Proof. Because of Lemma 3.2, we can assume without loss of generality that $\mathbf{f}_i = 0$. For each subdomain Ω_i , we multiply the definition of the discrete Neumann condition (2.8) by

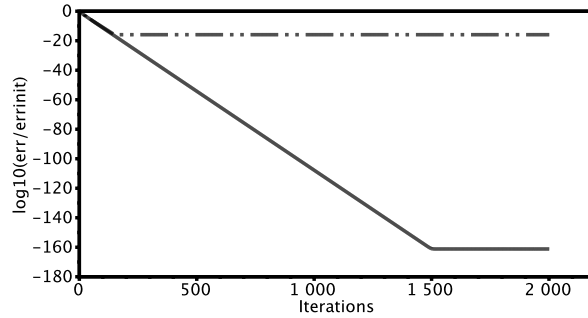


FIG. 3.1. Error using the OSM with auxiliary variables for 4×1 (solid) and 2×2 (dashed-dotted) subdomains.

$u_{i;j}$, then sum over all j such that \mathbf{x}_j belongs to $\bar{\Omega}_i$ to obtain

$$\begin{aligned}
 \int_{\Omega_i} |\nabla u_i^{n+1}|^2 + \eta \int_{\Omega_i} |u_i^{n+1}|^2 &= \sum_{\mathbf{x}_j \in \partial\Omega_i} \mathcal{N}_{i;j}^{n+1} u_{i;j}^{n+1} \\
 &= \sum_{i'} \sum_{\mathbf{x}_j \in \partial\Omega_i \cap \partial\Omega_{i'}} \mathcal{N}_{i,i';j}^{n+1} u_{i;j}^{n+1} && \text{(by (3.5))} \\
 &= \sum_{i'} \sum_{\mathbf{x}_j \in \partial\Omega_i \cap \partial\Omega_{i'}} \frac{|\mathcal{N}_{i,i';j}^{n+1} + \frac{p}{2} \sum_{j'} |\mathbf{x}_j - \mathbf{x}_{j'}| u_{i;j}^{n+1}|^2}{2p \sum_{j'} |\mathbf{x}_j - \mathbf{x}_{j'}|} \\
 &\quad - \frac{|\mathcal{N}_{i,i';j}^{n+1} - \frac{p}{2} \sum_{j'} |\mathbf{x}_j - \mathbf{x}_{j'}| u_{i;j}^{n+1}|^2}{2p \sum_{j'} |\mathbf{x}_j - \mathbf{x}_{j'}|}, \\
 &= \sum_{i'} \sum_{\mathbf{x}_j \in \partial\Omega_i \cap \partial\Omega_{i'}} \frac{|g_{i,i';j}^n|^2 - |g_{i,i';j}^{n+1}|^2}{2p \sum_{j'} |\mathbf{x}_j - \mathbf{x}_{j'}|} && \text{(by (3.4) and (3.3)).}
 \end{aligned}$$

We now sum over all subdomains i and over the iteration index n to get

$$\begin{aligned}
 \sum_{n=0}^N \sum_{i=1}^I \int_{\Omega_i} |\nabla u_i^{n+1}|^2 + \eta \int_{\Omega_i} |u_i^{n+1}|^2 &= \sum_{i,i'} \sum_{\mathbf{x}_j \in \partial\Omega_i \cap \partial\Omega_{i'}} \frac{|g_{i,i';j}^0|^2 - |g_{i,i';j}^{N+1}|^2}{2p \sum_{j'} |\mathbf{x}_j - \mathbf{x}_{j'}|} \\
 &\leq \sum_{i,i'} \sum_{\mathbf{x}_j \in \partial\Omega_i \cap \partial\Omega_{i'}} \frac{|g_{i,i';j}^0|^2}{2p \sum_{j'} |\mathbf{x}_j - \mathbf{x}_{j'}|}.
 \end{aligned}$$

This shows that the sum over the energy over all iterates and subdomains stays bounded as the iteration number N goes to infinity, which implies that the energy of the iterates and hence the iterates converge to zero. \square

3.2. Numerical observation using auxiliary variables. Using auxiliary variables can have surprising numerical side effects. In Figure 3.1 we display the error measured in the L^∞ -norm of the OSM with auxiliary variables for the domain $\Omega = (0, 4)^2$ decomposed once into 2×2 subdomains and once into 4×1 subdomains, for $p = 2.0$ and $\eta = 0.0$ and a mesh size $h = 1/10$. We iterate directly on the error equations, $f = 0$, and initialize the transmission conditions with random values (for the importance of random values, see [11]). We observe that in the presence of cross-points, convergence stagnates around machine precision, whereas without them, stagnation appears much later.

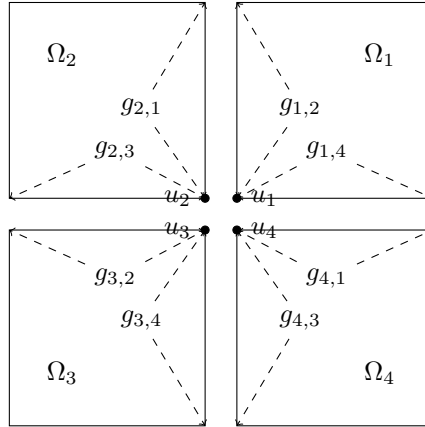


FIG. 3.2. *Degenerate case.*

To understand these results, we need to consider floating-point arithmetic (see [18, 20, 31]) and in particular the machine precision macheps and the smallest positive floating-point number minreal . In the above experiment we used double precision in C++, so $\text{macheps} = 2^{-53} \approx 1.1 \cdot 10^{-16}$ and $\text{minreal} \approx 4.9 \cdot 10^{-324}$. Had we been computing a real problem with nonzero right-hand side f , we would expect stagnation near machine precision. However, when iterating directly on the errors, stagnation should occur much later at the level of the smallest positive floating-point number.

To analyze the early stagnation observed, we consider a simple model problem with 2×2 subdomains (see Figure 3.2) where there is exactly one Q_1 -element per subdomain and the only interior node is a cross-point. This means that the mono-domain solution u is a scalar. We thus have $\Omega = (-h, h) \times (-h, h)$ and the subdomains $\Omega_1 = (0, h) \times (0, h)$, $\Omega_2 = (-h, 0) \times (0, h)$, $\Omega_3 = (-h, 0) \times (-h, 0)$, $\Omega_4 = (0, h) \times (-h, 0)$. We apply the OSM with lumped Robin transmission conditions and $f = 0$. Since there is only one interior node in the whole mesh, there is only a single test function ϕ with $\phi(x, y) = (1 - |x|)(1 - |y|)$. By (2.7), we have

$$\begin{aligned}
 A_1 = A_2 = A_3 = A_4 &= \eta h^2 \left(\int_0^1 (1-x)^2 dx \right)^2 + \int_0^1 (1-x)^2 dx + \int_0^1 (1-y)^2 dy \\
 &= \frac{\eta h^2}{9} + \frac{2}{3}.
 \end{aligned}$$

We use lumped Robin transmission conditions, and by (2.6), we get

$$B_1 = B_2 = B_3 = B_4 = \frac{p}{2} h \left(\int_0^1 (1-x) dx + \int_0^1 (1-y) dy \right) = ph.$$

Therefore, we have by (2.7) and (3.2)

$$u_i^{n+1} = \frac{g_i^{n+1}}{\frac{2}{3} + \frac{\eta h^2}{9} + ph}, \quad i = 1, \dots, 4.$$

Thus, for the OSM iteration, we obtain

$$(3.6) \quad \begin{aligned} u_1^{n+1} &= \frac{g_{12}^n + g_{14}^n}{\frac{2}{3} + \frac{\eta h^2}{9} + ph}, & u_2^{n+1} &= \frac{g_{23}^n + g_{21}^n}{\frac{2}{3} + \frac{\eta h^2}{9} + ph}, \\ u_3^{n+1} &= \frac{g_{32}^n + g_{34}^n}{\frac{2}{3} + \frac{\eta h^2}{9} + ph}, & u_4^{n+1} &= \frac{g_{43}^n + g_{41}^n}{\frac{2}{3} + \frac{\eta h^2}{9} + ph}, \end{aligned}$$

and by (3.3), we get

$$g_{i',i}^{n+1} := -g_{i,i'}^n + ph u_i^{n+1}.$$

Eliminating the variables u_i^{n+1} from the iteration leads to

$$\begin{bmatrix} g_{1,2}^{n+1} \\ g_{2,1}^{n+1} \\ g_{2,3}^{n+1} \\ g_{3,2}^{n+1} \\ g_{3,4}^{n+1} \\ g_{4,3}^{n+1} \\ g_{4,1}^{n+1} \\ g_{1,4}^{n+1} \end{bmatrix} = \begin{bmatrix} 0 & \alpha - 1 & \alpha & 0 & 0 & 0 & 0 & 0 \\ \alpha - 1 & 0 & 0 & 0 & 0 & 0 & 0 & \alpha \\ 0 & 0 & 0 & \alpha - 1 & \alpha & 0 & 0 & 0 \\ 0 & \alpha & \alpha - 1 & 0 & 0 & 0 & 0 & 0 \\ 0 & 0 & 0 & 0 & 0 & \alpha - 1 & \alpha & 0 \\ 0 & 0 & 0 & \alpha & \alpha - 1 & 0 & 0 & 0 \\ \alpha & 0 & 0 & 0 & 0 & 0 & 0 & \alpha - 1 \\ 0 & 0 & 0 & 0 & 0 & \alpha & \alpha - 1 & 0 \end{bmatrix} \begin{bmatrix} g_{1,2}^n \\ g_{2,1}^n \\ g_{2,3}^n \\ g_{3,2}^n \\ g_{3,4}^n \\ g_{4,3}^n \\ g_{4,1}^n \\ g_{1,4}^n \end{bmatrix},$$

where we introduced the scalar quantity

$$\alpha = \frac{ph}{\frac{\eta h^2}{9} + \frac{2}{3} + ph}.$$

Since $0 < \alpha < 1$, the ℓ^∞ -norm of this iteration matrix is 1, and hence its spectral radius is bounded by 1. Note however that 1 and -1 are eigenvalues of this matrix with the corresponding eigenvectors

$$(-1, 1, -1, 1, -1, 1, -1, 1)^T \quad \text{and} \quad (1, 1, -1, -1, 1, 1, -1, -1)^T.$$

This shows that the vector of auxiliary variables will not converge to 0 in general. However, the modes with eigenvalue $+1$ and -1 make no contribution to u_i , see (3.6), so in the algorithm, the iterates u_i^n will converge as proved in Theorem 3.3. In floating-point arithmetic however, the fact that the auxiliary variables do not converge (and remain $O(1)$ because of their initialization) prevents the algorithm applied to the error equations to converge in the iterates u_i^n below the machine precision as we observed in Figure 3.1. Luckily, this has no influence when solving a real problem with non-zero right-hand side but must be remembered when testing codes.

4. Complete communication. We now present a different approach not using auxiliary variables but still guaranteeing that the discrete mono-domain solution is a fixed-point of the discrete OSM. This requires the subdomains to communicate at cross-points with every subdomain sharing the cross-point. Most methods obtained algebraically using matrix splittings use complete communication. To get DDMs directly from the matrix, one usually duplicates the components corresponding to the nodes lying on the interfaces between the subdomains so that each node is present in the matrix as many times as the number of subdomains it belongs to; see for example [14, 27]. To obtain an *auxiliary variable method* instead of a *complete communication* from a matrix splitting, further duplication of nodal components would be necessary: nodal components would have to be duplicated as many times as the number of ordered pairs of distinct subdomains sharing at least one interface edge having that node as an endpoint. To prove convergence of this approach requires, however, other techniques than energy estimates; see [14, 27].

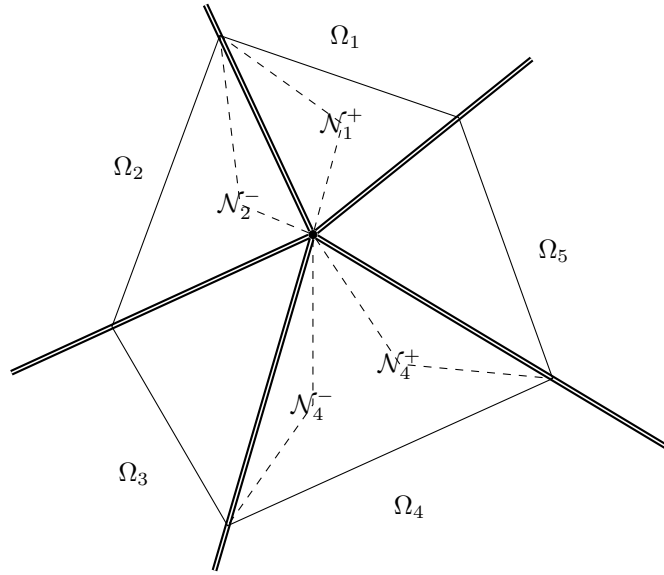


FIG. 4.1. Splitting of \mathcal{N}_i into \mathcal{N}_i^+ and \mathcal{N}_i^- .

4.1. Keeping the discrete mono-domain solution a fixed-point. Consider a cross-point \mathbf{x}_j belonging to the subdomains $\bar{\Omega}_i$, for i in $\{1, \dots, I\}$, with $I \geq 3$. We consider local linear updates for the discrete Robin transmission conditions at cross-points of the form

$$g_{i;j}^{n+1} = \ell_{\mathcal{D}}((u_{i;j}^n)_{1 \leq i \leq I}) + \ell_{\mathcal{N}}((\mathcal{N}_{i;j}(u_i))_{1 \leq i \leq I}),$$

where $\ell_{\mathcal{D}}$ and $\ell_{\mathcal{N}}$ are linear maps from \mathbb{R}^I to \mathbb{R}^I , which can be represented by matrices

$$\begin{bmatrix} g_{1;j}^{n+1} \\ \vdots \\ g_{I;j}^{n+1} \end{bmatrix} = \mathbf{A}_{\mathcal{D}} \begin{bmatrix} u_{1;j}^n \\ \vdots \\ u_{I;j}^n \end{bmatrix} + \mathbf{A}_{\mathcal{N}} \begin{bmatrix} \mathcal{N}_{1;j}^n \\ \vdots \\ \mathcal{N}_{I;j}^n \end{bmatrix}.$$

At the cross-point \mathbf{x}_j , the mono-domain solution satisfies (2.10), i.e.,

$$(4.1) \quad u_{i;j} = u_{1;j} \quad \text{for all } i \text{ in } \{1, \dots, I\}, \quad \sum_{i=1}^I \mathcal{N}_{i;j}(u_i) = 0.$$

For the mono-domain solution to be a fixed-point, $g_{i;j}^{n+1}$ should be equal to $g_{i;j}^n$ whenever the conditions (4.1) are satisfied. Therefore, the matrices must satisfy

$$(4.2) \quad (\mathbf{A}_{\mathcal{N}})_{ii'} = \delta_{i,i'} - \alpha_i, \quad \sum_{i'=1}^I (\mathbf{A}_{\mathcal{D}})_{ii'} = \frac{p}{2} \sum_{j' \text{ s.t. } [\mathbf{x}_j \mathbf{x}_{j'}] \text{ is a boundary edge of } \mathcal{T}_i} |\mathbf{x}_j - \mathbf{x}_{j'}|,$$

for some constants α_i .

4.2. An intuitive Neumann splitting near cross-points. Suppose we are given I values $(\mathcal{N}_i)_{i=1,\dots,I}$, each representing the discrete Neumann values at \mathbf{x}_j for the subdomain Ω_i . Our goal is to find a splitting $(\mathcal{N}_i^+, \mathcal{N}_i^-)_{i=1,\dots,I}$ such that

$$\mathcal{N}_i = \mathcal{N}_i^+ + \mathcal{N}_i^-.$$

There are obviously many such splittings. At the continuous level, the mono-domain solution has no Neumann jumps at the interface between subdomains. It thus makes sense, at an intuitive level, to search for a splitting minimizing the Neumann jumps $\mathcal{N}_{i+1}^- + \mathcal{N}_i^+$; see Figure 4.1. Therefore, we choose to minimize

$$\sum_{i=1}^I |\mathcal{N}_i^+ + \mathcal{N}_{i+1}^-|^2,$$

where by convention \mathcal{N}_{I+1}^- denotes \mathcal{N}_1^- . We will see that this still does not give a unique solution, but all such splittings give rise to the same transmission conditions in the OSM discretized by finite elements.

We denote by $\mathbf{a} \in \mathbb{R}^I$ the vector with $a_i = \mathcal{N}_i^-$, which implies $\mathcal{N}_i^+ = \mathcal{N}_i - a_i$. We thus search for \mathbf{a} in \mathbb{R}^I such that the function

$$\mathbf{a} \mapsto \sum_{i=1}^I |-a_i + \mathcal{N}_i + a_{i+1}|^2$$

is minimized, i.e., we want to compute the solution of

$$(4.3) \quad \operatorname{argmin}_{\mathbf{a} \in \mathbb{R}^I} \|\mathbf{L}\mathbf{a} - \mathcal{N}\|_2^2,$$

where the matrix $\mathbf{L} = (\ell_{ii'})_{1 \leq i, i' \leq I}$ is given by

$$\ell_{ij} = \begin{cases} 1 & \text{if } i' = i, \\ -1 & \text{if } i' = i + 1 \pmod I, \\ 0 & \text{otherwise,} \end{cases}$$

or more explicitly

$$\mathbf{L} = \begin{bmatrix} 1 & -1 & 0 & \dots & 0 & 0 \\ 0 & 1 & -1 & \ddots & \ddots & 0 \\ \vdots & \ddots & \ddots & \ddots & \ddots & \vdots \\ \vdots & \ddots & \ddots & \ddots & \ddots & \vdots \\ 0 & \ddots & \ddots & 0 & 1 & -1 \\ -1 & 0 & \dots & 0 & 0 & 1 \end{bmatrix}.$$

Equation (4.3) is a standard least-squares problem, but its solution is not unique since $\ker(\mathbf{L}) = \mathbb{R}[1, \dots, 1]^T$. If we require in addition that \mathbf{a} is orthogonal to $\ker(\mathbf{L})$, then \mathbf{a} is unique and

$$\mathbf{a} = \mathbf{L}^\dagger \mathcal{N},$$

where \mathbf{L}^\dagger is the pseudo-inverse of \mathbf{L} , and all the solutions to (4.3) are then of the form $\mathbf{L}^\dagger \mathcal{N} + \mathbb{R}[1, \dots, 1]^T$.

Since \mathbf{L} is a circulant matrix, its pseudo-inverse \mathbf{L}^\dagger is too. Let $(\mu_i)_{i \in \mathbb{Z}}$ be I -periodic such that $\ell_{ii'}^\dagger = \mu_{i'-i}$, which implies

$$\mathbf{L}^\dagger = \begin{bmatrix} \mu_0 & \mu_1 & \cdots & \mu_{I-1} \\ \mu_{I-1} & \mu_0 & \ddots & \vdots \\ \vdots & \ddots & \ddots & \mu_1 \\ \mu_1 & \cdots & \mu_{I-1} & \mu_0 \end{bmatrix}.$$

In addition, since $\ker(\mathbf{L}) = \mathbb{R}[1, \dots, 1]^T$, we have

$$\mathbf{L}^\dagger \mathbf{L} = \mathbf{I} - \frac{1}{I} \begin{bmatrix} 1 & \cdots & 1 \\ \vdots & \ddots & \vdots \\ 1 & \cdots & 1 \end{bmatrix},$$

and hence,

$$\mu_0 - \mu_{I-1} = 1 - \frac{1}{I} \quad \text{and} \quad \mu_i - \mu_{i-1} = -\frac{1}{I} \quad \text{for all } 1 \leq i \leq I.$$

Therefore, for all $i = 0, \dots, I-1$, we get

$$\mu_i = \mu_0 - \frac{i}{I}.$$

Moreover, $\text{range}(\mathbf{L}^\dagger) = \ker(\mathbf{L})^\perp$ implies $\sum_{i=0}^{I-1} \mu_i = 0$, which yields $\mu_0 = \frac{I-1}{2}$. Hence, for all $i = 0, \dots, I-1$,

$$\mu_i = \frac{I-1}{2} - \frac{i}{I}.$$

We thus obtain for the solution of the least squares problem

$$a_i = \sum_{i'=1}^I \mu_{i'-i} \mathcal{N}_{i'},$$

which gives for the splitting of the Neumann values

$$\mathcal{N}_i^+ = \sum_{i'=1}^I \mu_{i'-i} \mathcal{N}_{i'}, \quad \mathcal{N}_i^- = \mathcal{N}_i - \sum_{i'=1}^I \mu_{i'-i} \mathcal{N}_{i'}.$$

We can use this splitting now in the OSM to exchange the Neumann contributions \mathcal{N}_i^+ and \mathcal{N}_{i+1}^- in the Robin transmission conditions, i.e., we set

$$\begin{aligned} (\mathbf{A}_{\mathcal{N}} \mathcal{N})_i &= -\mathcal{N}_{i+1}^- - \mathcal{N}_{i-1}^+ \\ &= -\mathcal{N}_{i-1} + \sum_{i'=1}^I \mu_{i'-i+1} \mathcal{N}_{i'} - \sum_{i'=1}^I \mu_{i'-i-1} \mathcal{N}_{i'} \\ &= -\mathcal{N}_{i-1} + \sum_{i'=1}^I (\mu_{i'-i+1} - \mu_{i'-i-1}) \mathcal{N}_{i'}. \end{aligned}$$

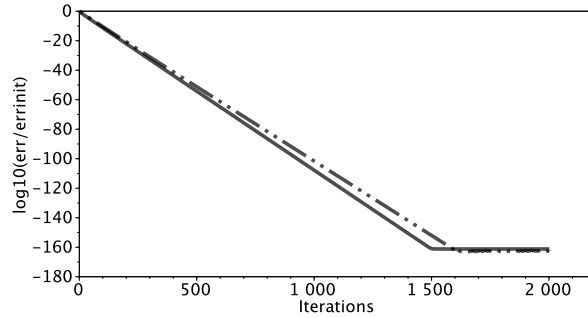


FIG. 4.2. Numerical convergence of complete communication for 4×1 (solid) and 2×2 (dashed-dotted) subdomains.

We have

$$\mu_{i'-i+1} - \mu_{i'-i-1} = \begin{cases} 1 - \frac{2}{I} & \text{if } i' = i \pmod I, \\ 1 - \frac{2}{I} & \text{if } i' = i - 1 \pmod I, \\ -\frac{2}{I} & \text{otherwise.} \end{cases}$$

Therefore, we set

$$(\mathbf{A}_{\mathcal{N}}\mathcal{N})_i = \mathcal{N}_i - \frac{2}{I} \sum_{i'=1}^I \mathcal{N}_{i'}.$$

4.3. An intuitive splitting of the Dirichlet part. We must choose a matrix $\mathbf{A}_{\mathcal{D}}$ satisfying (4.2), i.e.,

$$\sum_{i'=1}^I (\mathbf{A}_{\mathcal{D}})_{ii'} = \frac{p}{2} \sum_{\substack{j', \mathbf{x}_{j'} \in \partial\Omega_i, \\ [\mathbf{x}_j \mathbf{x}_{j'}] \text{ edge of } \mathcal{T}_i}} |\mathbf{x}_j - \mathbf{x}_{j'}|.$$

There are also many possible choices for $(\mathbf{A}_{\mathcal{D}})_{ii'}$, but in contrast to the Neumann conditions, which are only known variationally, the Dirichlet values are known on the boundary. Therefore, to split the sum of $|\mathbf{x}_j - \mathbf{x}_{j'}|$, we look at which neighbouring subdomain the edge $[\mathbf{x}_j \mathbf{x}_{j'}]$ belongs to: if one is $\bar{\Omega}_i$ and the other is $\bar{\Omega}_{i'}$, then we put $p|\mathbf{x}_j - \mathbf{x}_{j'}|$ into $(\mathbf{A}_{\mathcal{D}})_{ii'}$. Hence, we set

$$(\mathbf{A}_{\mathcal{D}})_{ii'} = \begin{cases} \frac{p}{2} \sum_{\substack{j', \mathbf{x}_{j'} \in \partial\Omega_i \cap \partial\Omega_{i'}, \\ [\mathbf{x}_j \mathbf{x}_{j'}] \text{ edge of both } \mathcal{T}_i \text{ and } \mathcal{T}_{i'}}} |\mathbf{x}_j - \mathbf{x}_{j'}| & \text{if } i' \neq i, \\ 0 & \text{if } i' = i. \end{cases}$$

4.4. Numerical simulations. We do the same experiment with complete communication as we did for the auxiliary variable method in Section 3.2. The results are shown in Figure 4.2. As expected, for complete communication, convergence is also observed up to the square root of `minreal` for the 2×2 subdomain cases, i.e., when there are cross-points. In practice, when using complete communication, the Robin parameters should be different at cross-points; see [14] for details. In this paper, we chose not to do so and use the same p at cross-points.

5. Conclusion. This paper contains two concrete propositions on how to discretize Neumann conditions at cross-points in domain decomposition methods: the auxiliary variable method and complete communication. We showed three new results: first, that the introduction of auxiliary variables makes it possible to prove convergence of the discretized methods for very general decompositions, including cross-points, using energy estimates. Second, that Neumann conditions can be split at cross-points in a way minimizing artificial oscillation in the domain decomposition, and third, in the Appendix, that lumping the mass matrix in a finite element-discretized optimized Schwarz method leads to better performance. We explained this by a reinterpretation at the continuous level, which shows a tangential higher-order operator appearing. Its weight can even be optimized using the new concept of overlumping, and this can be done purely at the algebraic level without need to discretize a complicated higher-order operator.

We explained the auxiliary variable method and complete communication for the concrete example of optimized Schwarz methods, but whenever an iterative domain decomposition method requires the computation of Neumann contributions at cross-points, the discrete version of the algorithm will not be a straightforward adaptation of the continuous version of the algorithm, and one can consider to use the auxiliary variable method or complete communication. Complete communication can always be used since it does not need to split Neumann contributions along edges. Applying the auxiliary variable method can be trickier as it requires the existence of an updating formula for the split quantities themselves. Advantages of the auxiliary variable method are the existence of a convergence theorem and that it is easier to program due to less direct communication needed between computational units. An advantage of complete communication is that the iterates do not depend on additional variables. The numerical results in Tables A.2 and A.3 do not show any significant convergence advantage for one method over the other.

We have only considered one-level domain decomposition methods here, but since two-level methods are in general based on one-level methods, both approaches of dealing with the Neumann contribution near cross-points can be applied to the one-level step of the two-level method. We have also restricted our presentation to two spatial dimensions. In higher dimensions, in addition to cross-points, there would also be cross-edges. Both the auxiliary variable method and complete communication can be adapted to higher dimensions, which is work in progress.

Acknowledgements. This study has been carried out with financial support from the French State, managed by the French National Research Agency (ANR) in the frame of the "Investments for the future" Programme IdEx Bordeaux–CPU (ANR-10-IDEX-03-02).

Appendix A. (Over)lumping of the interface mass matrix. We start with a numerical experiment using the consistent interface mass matrix B_i from (2.5) and the lumped interface mass matrix B_i^{lump} from (2.6) in the Robin transmission condition of the OSM. We solve the Poisson equation with right-hand side $f(x, y) = 2(y(4.0 - y) + x(4.0 - x))$ on the square domain $\Omega = (0, 4)^2$ with 3×3 subdomains of equal size and Robin parameter $p = 2.0$ discretized using Q_1 -finite elements with mesh size $h = 1/15$. Figure A.1 shows how the error decreases as a function of the iteration index in the OSM for these two choices. We see that initially the two methods converge at the same rate, but around iteration 40, the method using the consistent mass interface matrix slows down. We display in Figure A.2 snapshots of the error distribution for selected iteration indices. We see that a highly oscillatory mode appears in the error along the interfaces. Snapshots of the error distribution using the lumped mass matrix B_i^{lump} are presented in Figure A.3 for the same experimental setting. We see that with the lumped mass matrix, the high-frequency error mode along the interface is much less pronounced and convergence is faster.

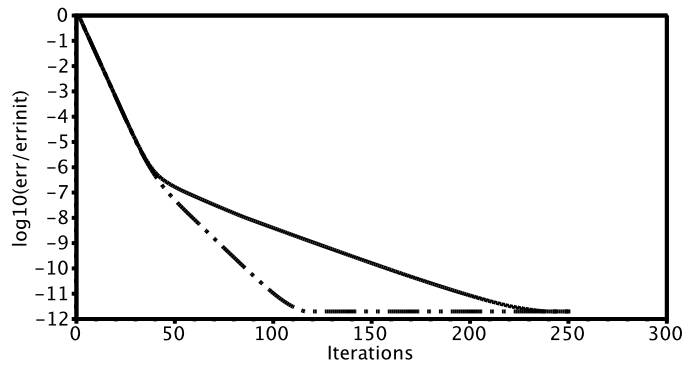


FIG. A.1. Convergence with lumped Robin(dashed-dotted) and consistent Robin(solid).

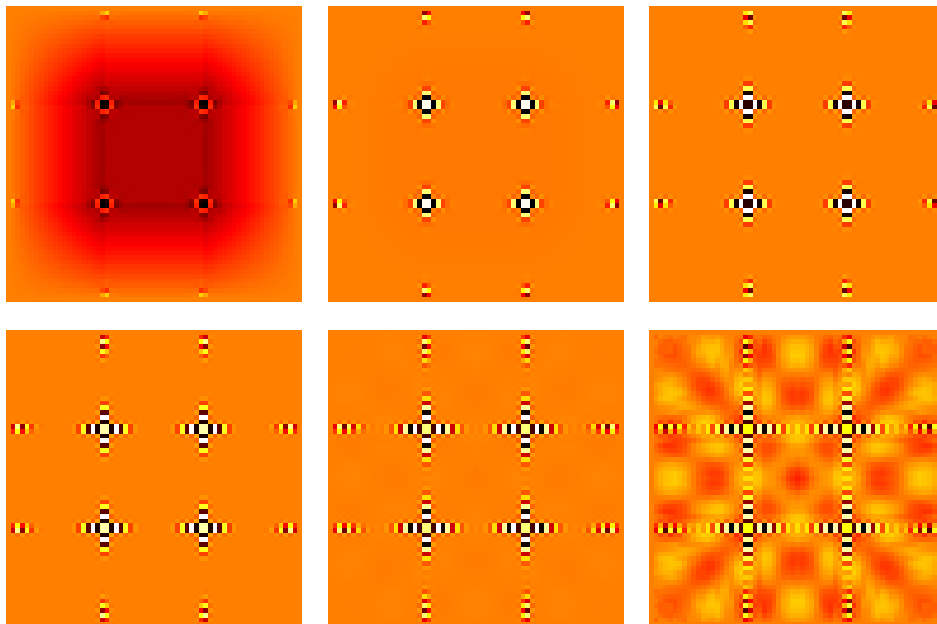


FIG. A.2. Scaled error distribution at iteration 35, 50, 75, 100, 150, and 200 for the OSM with consistent interface mass matrix using auxiliary variables at cross-points.

In order to understand this phenomenon, we reinterpret the effect of mass lumping at the continuous level: the difference

$$B_{i;j,j'}^{\text{lump}} - B_{i;j,j'} = \begin{cases} \frac{\rho}{6} \sum_{j''} |\mathbf{x}_{i;j} - \mathbf{x}_{i;j''}| & \text{if } j' = j \text{ and } \mathbf{x}_{i;j} \text{ lies on } \partial\Omega_i, \\ -\frac{\rho}{6} |\mathbf{x}_{i;j} - \mathbf{x}_{i;j'}| & \text{if } [\mathbf{x}_{i;j} \mathbf{x}_{i;j'}] \text{ is an edge of } \partial\Omega_i, \\ 0 & \text{otherwise,} \end{cases}$$

looks like the discretization of a negative one-dimensional Laplacian. Technically, this holds true only if the step size h is constant and we are not at a cross-point. In that case, the lumped

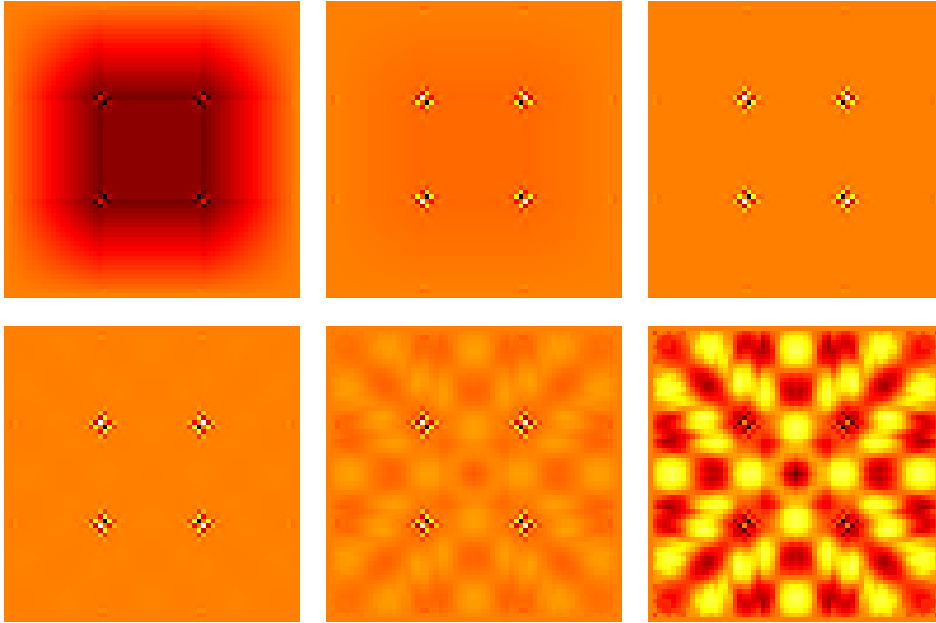


FIG. A.3. Scaled error distribution at iteration 35, 50, 65, 80, 95, 110 for the OSM with lumped interface mass matrix using auxiliary variables at cross-points.

matrix actually discretizes the higher-order transmission condition

$$\frac{\partial u}{\partial \mathbf{n}_i} - \frac{ph^2}{6} \frac{\partial^2 u}{\partial^2 \tau} + pu.$$

If we could modify the value of ph^2 , we would obtain a truly optimizable higher-order, or Ventcell, transmission condition. This motivates the idea of overlumping: introducing a relaxation parameter ω , we define

$$B_{i;j,j'}^\omega := (1 - \omega)B_{i;j,j'} + \omega B_{i;j,j'}^{\text{lump}}$$

and thus obtain a discretization of the transmission condition

$$\frac{\partial u}{\partial \mathbf{n}_i} - \omega \frac{ph^2}{6} \frac{\partial^2 u}{\partial^2 \tau} + pu.$$

We perform now a numerical experiment with this overlumped mass matrix. For a rectangular domain $\Omega = (0, 4) \times (0, 2)$ with two square subdomains $\Omega_1 = (0, 2) \times (0, 2)$ and $\Omega_2 = (2, 4) \times (0, 2)$, we run the OSM on Laplace's equation discretized with Q_1 -finite elements and homogeneous boundary conditions, thus simulating directly the error equations. We start with a random initial guess on the interface $\{2\} \times (0, 2)$ (for the importance of random values, see [11]). We apply 50 optimized Schwarz iterations. We do this for 10×10 , 20×20 , 50×50 , and 100×100 cells per subdomains with the Robin parameter p ranging from 1 to 20 with an increment of 0.5 and the lump parameter ω from 0 to 100 with an increment of 0.25. We present the optimal p and ω in Table A.1. Using the asymptotic results from [10], the optimal asymptotic choice of p for the consistent mass interface matrix should behave like $p = O(1/h^{1/2})$, and in the emulated Ventcell case from overlumping, we should have $p = O(1/h^{1/4})$ and $\omega = O(1/h)$, which is well what we observe.

TABLE A.1

Optimal Robin parameter p and overlumping factor ω with corresponding numerical convergence factor $\kappa = \exp(\log(\|u_{50}\|_\infty/\|u_0\|_\infty)/50)$ and 2 subdomains.

Cells in Ω_i	Consistent	Lumped	Best
10×10	$\omega = 0.0, p = 6.0,$ $\kappa = 0.5791628$	$\omega = 1.0, p = 3.5,$ $\kappa = 0.3887587$	$\omega = 10.25, p = 1.5,$ $\kappa = 0.1245496$
20×20	$\omega = 0.0, p = 8.5,$ $\kappa = 0.6853493$	$\omega = 1.0, p = 5.0,$ $\kappa = 0.5222360$	$\omega = 17.75, p = 2.0,$ $\kappa = 0.1852617$
50×50	$\omega = 0.0, p = 14.0,$ $\kappa = 0.7847913$	$\omega = 1.0, p = 8.0,$ $\kappa = 0.6643391$	$\omega = 45.0, p = 2.5,$ $\kappa = 0.2863597$
100×100	$\omega = 0.0, p = 22.5,$ $\kappa = 0.8141025$	$\omega = 1.0, p = 12.0,$ $\kappa = 0.7332624$	$\omega = 89.25, p = 3.0,$ $\kappa = 0.3571062$

TABLE A.2

Optimal Robin parameter p and overlumping factor ω with corresponding numerical convergence factor $\kappa = \exp(\log(\|u_{60}\|_\infty/\|u_{30}\|_\infty)/30)$ for 2×2 subdomains using the auxiliary variable method.

Cells in Ω_i	Consistent	Lumped	Best
10×10	$\omega = 0.0, p = 3.5,$ $\kappa = 0.7468911$	$\omega = 1.0, p = 2.0,$ $\kappa = 0.6833862$	$\omega = 17.25, p = 0.8,$ $\kappa = 0.4862979$
20×20	$\omega = 0.0, p = 5.0,$ $\kappa = 0.8073780$	$\omega = 1.0, p = 3.0,$ $\kappa = 0.7053783$	$\omega = 14.75, p = 1.5,$ $\kappa = 0.5045374$
50×50	$\omega = 0.0, p = 8.0,$ $\kappa = 0.8775996$	$\omega = 1.0, p = 4.5,$ $\kappa = 0.8032485$	$\omega = 82.0, p = 1.5,$ $\kappa = 0.5001431$
100×100	$\omega = 0.0, p = 11.0,$ $\kappa = 0.9102802$	$\omega = 1.0, p = 6.5,$ $\kappa = 0.8547884$	$\omega = 122.5, p = 2.0,$ $\kappa = 0.6013464$

We perform a new numerical experiment with this overlumped mass matrix but in the presence of a single cross-point. For this experiment, we use the auxiliary variable method, see Table A.2, and complete communication³; see Table A.3. For a square domain $\Omega = (0, 4) \times (0, 4)$ with four square subdomains $\Omega_1 = (0, 2) \times (0, 2)$, $\Omega_2 = (2, 4) \times (0, 2)$, $\Omega_3 = (0, 2) \times (2, 4)$, and $\Omega_4 = (2, 4) \times (2, 4)$, we run the OSM on Laplace's equation discretized with Q_1 -finite elements and homogeneous boundary conditions, thus simulating directly the error equations. Starting with a random initial guess on the interface $\{2\} \times (0, 4) \cup (0, 4) \times \{2\}$, we apply 50 optimized Schwarz iterations. We do this for 10×10 , 20×20 , 50×50 , and 100×100 cells per subdomains. We start with the Robin parameter p ranging from 1 to 20 with an increment of 0.5 and the lump parameter ω from 0 to 100 with an increment of 0.25. For the case of 100×100 cells per subdomain with consistent Robin conditions, we extended the search for the Robin parameter up to 24.5. For the best (overlumping) case with 2×2 subdomains and 10×10 cells per subdomain, we extended the search for the optimal p to the interval $[0.1, 1]$ with an increment of 0.1.

Appendix B. A simple lemma on connected graphs.

LEMMA B.1. *Let \mathcal{G} be a connected graph. Let $V(\mathcal{G})$ be its set of vertices and $E(\mathcal{G})$ be its set of edges. Let ϕ be a function from $V(\mathcal{G})$ to \mathbb{R} such that $\sum_{v \in V(\mathcal{G})} \phi(v) = 0$. Let*

$$E_f(\mathcal{G}) = \{(v_1, v_2) \in V(\mathcal{G}) \times V(\mathcal{G}) \text{ s.t. } \{v_1, v_2\} \in E(\mathcal{G})\}.$$

³Using $\mathbf{A}_{\mathcal{D}}$ and $\mathbf{A}_{\mathcal{N}}$ of Section 4.2 and Section 4.2.

TABLE A.3

Optimal Robin parameter p and overlumping factor ω with corresponding numerical convergence factor $\kappa = \exp(\log(\|u_{60}\|_\infty/\|u_{30}\|_\infty)/30)$ for 2×2 subdomains using complete communication. Same p at the cross-point as on the edge.

Cells in Ω_i	Consistent	Lumped	Best
10×10	$\omega = 0.0, p = 3.5,$ $\kappa = 0.7553129$	$\omega = 1.0, p = 2.0,$ $\kappa = 0.6967638$	$\omega = 17.75, p = 1.0,$ $\kappa = 0.3989268$
20×20	$\omega = 0.0, p = 5.0,$ $\kappa = 0.8134911$	$\omega = 1.0, p = 3.0,$ $\kappa = 0.7082014$	$\omega = 15.0, p = 1.5,$ $\kappa = 0.4997952$
50×50	$\omega = 0.0, p = 8.0,$ $\kappa = 0.8778605$	$\omega = 1.0, p = 4.5,$ $\kappa = 0.8034476$	$\omega = 86.0, p = 1.5,$ $\kappa = 0.5141311$
100×100	$\omega = 0.0, p = 11.0,$ $\kappa = 0.9106798$	$\omega = 1.0, p = 6.5,$ $\kappa = 0.8528811$	$\omega = 122.0, p = 2.0,$ $\kappa = 0.6006753.$

Then, there exists a function

$$\psi: E_f(G) \rightarrow \mathbb{R}$$

such that

$$\begin{aligned} \psi(v_1, v_2) &= -\psi(v_2, v_1) \quad \text{for all } (v_1, v_2) \text{ in } E_f(G), \\ \phi(v_1) &= \sum_{v_2 \text{ s.t. } (v_1, v_2) \text{ in } E_f(G)} \psi(v_1, v_2). \end{aligned}$$

Proof. The proof is based on recurrence over the number of vertices. The lemma is trivially true when the number of vertices is 1. Suppose the lemma is true when the number of vertices is n with $n \geq 1$. Let G be a connected graph with $n + 1$ vertices. It is well known that there exists a vertex v such that $G - \{v\}$ remains connected; see [33, Exercise 1.3.38]. Since G is connected, there are edges of G originating from v . Choose w_0 adjacent to v . Set $\psi(v, w_0) := \phi(v)$, $\psi(w_0, v) := -\phi(v)$, and $\psi(v, w) := \psi(w, v) := 0$ for all other vertices w adjacent to v . Set

$$\begin{aligned} \hat{\phi}: V(G) \setminus \{v\} &\rightarrow \mathbb{R} \\ w &\mapsto \begin{cases} \phi(w) & \text{if } w \text{ not adjacent to } v, \\ \phi(w) - \psi(w, v) & \text{if } w \text{ adjacent to } v. \end{cases} \end{aligned}$$

We have $\sum_w \hat{\phi}(w) = \sum_w \phi(w) = 0$. We apply the lemma to $\hat{\phi}$ and $G - \{v\}$ which is connected and get the remaining values of ψ . \square

REFERENCES

- [1] A. BENDALI AND Y. BOUBENDIR, *Non-overlapping domain decomposition method for a nodal finite element method*, Numer. Math., 103 (2006), pp. 515–537.
- [2] B. BIALECKI AND M. DRYJA, *Nonoverlapping domain decomposition with cross points for orthogonal spline collocation*, J. Numer. Math., 16 (2008), pp. 83–106.
- [3] Y. BOUBENDIR, A. BENDALI, AND M. B. FARES, *Coupling of a non-overlapping domain decomposition method for a nodal finite element method with a boundary element method*, Internat. J. Numer. Methods Engrg., 73 (2008), pp. 1624–1650.
- [4] R. CAUTRÈS, R. HERBIN, AND F. HUBERT, *The Lions domain decomposition algorithm on non-matching cell-centred finite volume meshes*, IMA J. Numer. Anal., 24 (2004), pp. 465–490.

- [5] P. CHEVALIER AND F. NATAF, *Symmetrized method with optimized second-order conditions for the Helmholtz equation*, in Domain Decomposition Methods 10, J. Mandel, C. Farhat, and X.-C. Cai, eds., vol. 218 of Contemp. Math., Amer. Math. Soc., Providence, 1998, pp. 400–407.
- [6] B. DESPRÉS, *Domain decomposition method and the Helmholtz problem*, in Mathematical and Numerical Aspects of Wave Propagation Phenomena (Strasbourg, 1991), G. Cohen, L. Halpern, and P. Joly, eds., SIAM, Philadelphia, 1991, pp. 44–52.
- [7] V. DOLEAN AND M. J. GANDER, *Can the discretization modify the performance of Schwarz methods?*, in Domain Decomposition Methods in Science and Engineering XIX, Y. Huang, R. Kornhuber, O. Widlund, and J. Xu, eds., vol. 78 of Lect. Notes Comput. Sci. Eng., Springer, Heidelberg, 2011, pp. 117–124.
- [8] M. DRYJA, W. PROSKUROWSKI, AND O. WIDLUND, *A method of domain decomposition with crosspoints for elliptic finite element problems*, in Optimal Algorithms, B. Sendov, ed., Bulgarian Academy of Sciences, Sofia, 1986, pp. 97–111.
- [9] C. FARHAT, M. LESOINNE, P. LE TALLEC, K. PIERSON, AND D. RIXEN, *FETI-DP: A Dual-Primal unified FETI method - part I: A faster alternative to the two-level FETI method*, Internat. J. Numer. Methods Engrg., 50 (2001), pp. 1523–1544.
- [10] M. J. GANDER, *Optimized Schwarz methods*, SIAM J. Numer. Anal., 44 (2006), pp. 699–731.
- [11] ———, *Schwarz methods over the course of time*, Electron. Trans. Numer. Anal., 31 (2008), pp. 228–255. <http://etna.mcs.kent.edu/vol.31.2008/pp228-255.dir/pp228-255.pdf>
- [12] M. J. GANDER, L. HALPERN, AND F. NATAF, *Optimized Schwarz methods*, in Domain Decomposition Methods in Sciences and Engineering (Chiba, 1999), T. Chan, T. Kako, H. Kawarada, and O. Pironneau, eds., DDM.org, Augsburg, 2001, pp. 15–27.
- [13] M. J. GANDER, F. HUBERT, AND S. KRELL, *Optimized Schwarz algorithm in the framework of DDV schemes*, in Domain Decomposition Methods in Science and Engineering XXI, J. Erhel, M. J. Gander, L. Halpern, G. Pichot, T. Sassi, and O. Widlund, eds., vol. 98 of Lect. Notes Comput. Sci. Eng., Springer Int. Publ, Switzerland, 2014, pp. 457–466.
- [14] M. J. GANDER AND F. KWOK, *Best Robin parameters for optimized Schwarz methods at cross points*, SIAM J. Sci. Comput., 34 (2012), pp. A1849–A1879.
- [15] ———, *On the applicability of Lions’ energy estimates in the analysis of discrete optimized Schwarz methods with cross points*, in Domain Decomposition Methods in Science and Engineering XX, R. E. Bank, M. Holst, O. Widlund, and J. Xu, eds., vol. 91 of Lect. Notes Comput. Sci. Eng., Springer, Heidelberg, 2013, pp. 475–483.
- [16] M. J. GANDER, F. KWOK, AND K. SANTUGINI, *Optimized Schwarz methods at cross points: the finite volume case*, in preparation, 2016.
- [17] M. J. GANDER, F. MAGOULÈS, AND F. NATAF, *Optimized Schwarz methods without overlap for the Helmholtz equation*, SIAM J. Sci. Comput., 24 (2002), pp. 38–60.
- [18] D. GOLDBERG, *What every computer scientist should know about floating point arithmetic*, ACM Computing Surveys, 23 (1991), pp. 5–48.
- [19] L. HALPERN AND F. HUBERT, *A finite volume Ventcell-Schwarz algorithm for advection-diffusion equations*, SIAM J. Numer. Anal., 52 (2014), pp. 1269–1291.
- [20] IEEE, *IEEE Standard for Floating-Point Arithmetic*, The Institute of Electrical and Electronics Engineers, New York, August 2008.
- [21] C. JAPHET, *Conditions aux limites artificielles et décomposition de domaine: Méthode O02 (optimisé d’ordre 2). Application à la résolution de problèmes en mécanique des fluides*, Tech. Report 373, CMAP (Ecole Polytechnique), 1997.
- [22] ———, *Optimized Krylov-Ventcell method. Application to convection-diffusion problems*, in Proceedings of the 9th International Conference on Domain Decomposition Methods, P. E. Bjørstad, M. S. Espedal, and D. E. Keyes, eds., ddm.org, 1998, pp. 382–389.
- [23] C. JAPHET AND F. NATAF, *The best interface conditions for domain decomposition methods: absorbing boundary conditions*, in Absorbing Boundaries and Layers, Domain Decomposition Methods, L. Tourrette and L. Halpern, eds., Nova Sci. Publ., Huntington, 2001, pp. 348–373.
- [24] C. JAPHET, F. NATAF, AND F. ROGIER, *The optimized order 2 method. Application to convection-diffusion problems*, Future Generation Comp. Sys., 18 (2001), pp. 17–30.
- [25] A. KLawonn, O. B. WIDLUND, AND M. DRYJA, *Dual-primal FETI methods for three-dimensional elliptic problems with heterogeneous coefficients*, SIAM J. Numer. Anal., 40 (2002), pp. 159–179.
- [26] P.-L. LIONS, *On the Schwarz alternating method. III. A variant for nonoverlapping subdomains*, in Third International Symposium on Domain Decomposition Methods for Partial Differential Equations, T. Chan, R. Glowinski, J. Periaux, and O. Widlund, eds., SIAM, Philadelphia, 1990, pp. 202–223.
- [27] S. LOISEL, *Condition number estimates for the nonoverlapping optimized Schwarz method and the 2-Lagrange multiplier method for general domains and cross points*, SIAM J. Numer. Anal., 51 (2013), pp. 3062–3083.
- [28] J. MANDEL AND M. BREZINA, *Balancing domain decomposition for problems with large jumps in coefficients*, Math. Comp., 65 (1996), pp. 1387–1401.
- [29] A. QUARTERONI AND A. VALLI, *Domain Decomposition Methods for Partial Differential Equations*, Oxford

- University Press, New York, 1999.
- [30] B. F. SMITH, P. E. BJØRSTAD, AND W. GROPP, *Domain Decomposition: Parallel Multilevel Methods for Elliptic Partial Differential Equations*, Cambridge University Press, Cambridge, 1996.
 - [31] P. H. STERBENZ, *Floating-Point Computation*, Prentice-Hall, Englewood Cliffs, 1974.
 - [32] A. TOSELLI AND O. WIDLUND, *Domain Decomposition Methods—Algorithms and Theory*, Springer, Berlin, 2005.
 - [33] D. B. WEST, *Introduction to Graph Theory*, 2nd ed., Prentice Hall, Englewood Cliffs, 2000.